NANO · MICRO small

Supporting Information

for *Small*, DOI 10.1002/smll.202404963

Injectable PLGA Microscaffolds with Laser-Induced Enhanced Microporosity for Nucleus Pulposus Cell Delivery

Paweł Nakielski, Alicja Kosik-Kozioł, Chiara Rinoldi, Daniel Rybak, Namdev More, Jacob Wechsler, Tomasz P. Lehmann, Maciej Głowacki, Bogusz Stępak, Magdalena Rzepna, Martina Marinelli, Massimiliano Lanzi, Dror Seliktar, Sarah Mohyeddinipour, Dmitriy Sheyn and Filippo Pierini**

Supporting Information

Injectable PLGA microscaffolds with laser-induced enhanced microporosity for nucleus pulposus cell delivery

Paweł Nakielski, Alicja Kosik-Kozioł, Chiara Rinoldi, Daniel Rybak, Namdev More, Jacob Wechsler, Tomasz P. Lehmann, Maciej Głowacki, Bogusz Stępak, Magdalena Rzepna, Martina Marinelli, Massimiliano Lanzi, Dror Seliktar, Sarah Mohyeddinipour, Dmitriy Sheyn and Filippo Pierini**

1. The effect of different pore-forming techniques on nanofibers morphology.

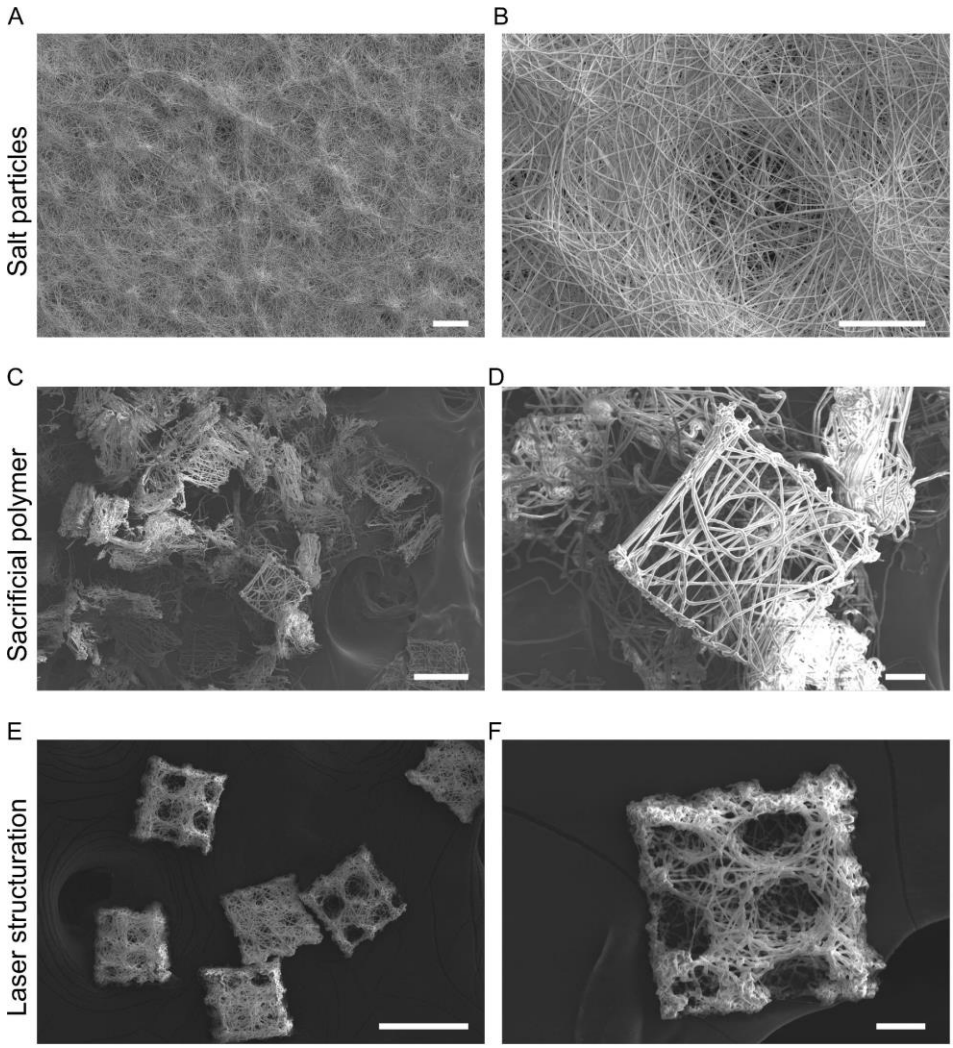

Figure S1. Comparison between different methods of pores formation. A) Salt particles were ground and suspended in ethanol solution and then added to the electrospun mat during electrospinning multiple times. B) Close view of the pore and morphology of the fibers around

salt particles. C) MS after sacrificial polymer removal showing gluing of microscaffolds. D) Close view at the MS showing skeleton after sacrificial polymer removal. E) Single MSP after femtosecond laser structuration. F) Close view at the MSP showing regularly structured pores.

2. **The effect of different laser types on the quality of the structuration at the MS edge.**

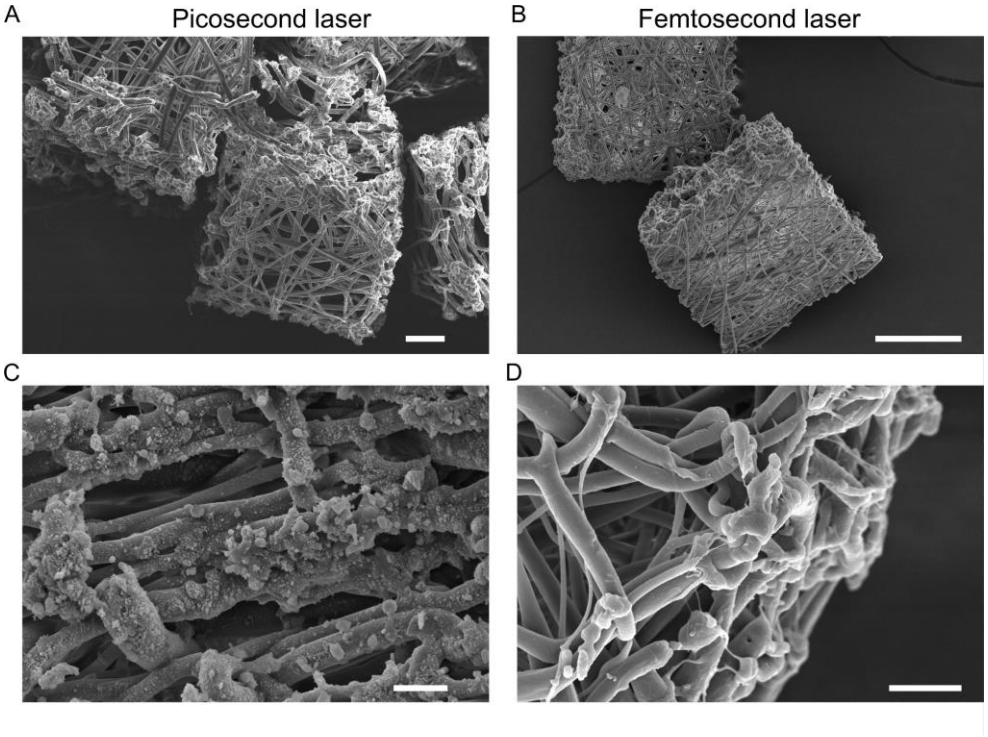

Figure S2. Comparison between picosecond and femtosecond laser ablation. A) Morphology of MS structured with picosecond laser. Scale bar 20 μm. B) Morphology of MS structured with a femtosecond laser. Scale bar 50 μm. C) Close view at the edge of picosecond laser-structured MS. Scale bar 2 μm. D) Close view at the edge of femtosecond laser-structured MS. Scale bar 2 μm.

3. Injection force of the MS, MSP suspended in hyaluronic acid and control

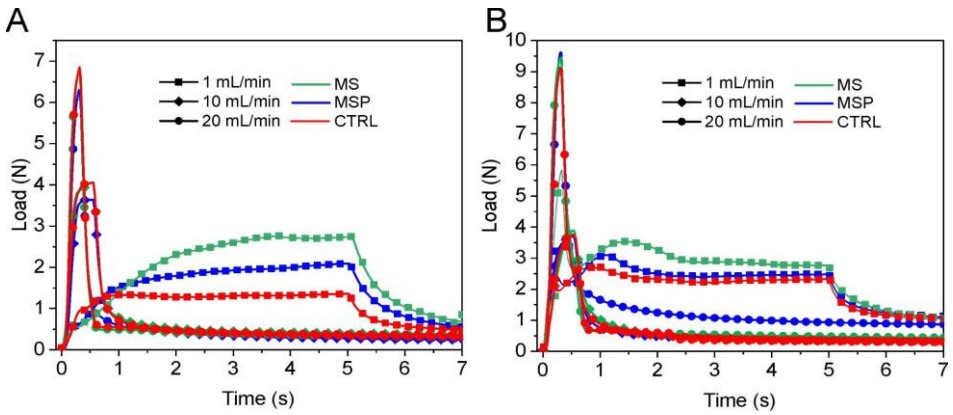

Figure S3. Injection force of the MS, MSP suspended in 0.5% hyaluronic acid and control (0.5% hyaluronic acid) A) Needle outlet in the air. B) Needle inserted into 7% PAAm hydrogel cube.

4. Gel Permeation Chromatography of PLGA microscaffolds before and after gamma irradiation

Table S1. Molecular weight and polydispersity index of electrospun PLGA nanofibers before and after gamma irradiation and porosity formation (MSP).

Group	Mn (g/mol)	Mw (g/mol)	PDI (polydispersity index)
MS	141000	178000	1.26
MSP	132500	180000	1.36
MS IRR	79000	116000	1.48
MSP IRR	59000	100000	1.69

5. PAAm hydrogel stiffness measurements

The compression tests on hydrogels were conducted using the texture analyzer (CTX TA, Brookfield Ametek), with a 50 N load cell and maintaining a constant rate of 1 mm min^{-1}. The compressive modulus was calculated through linear regression applied to the stress–strain curve within the 10 to 15% strain range.

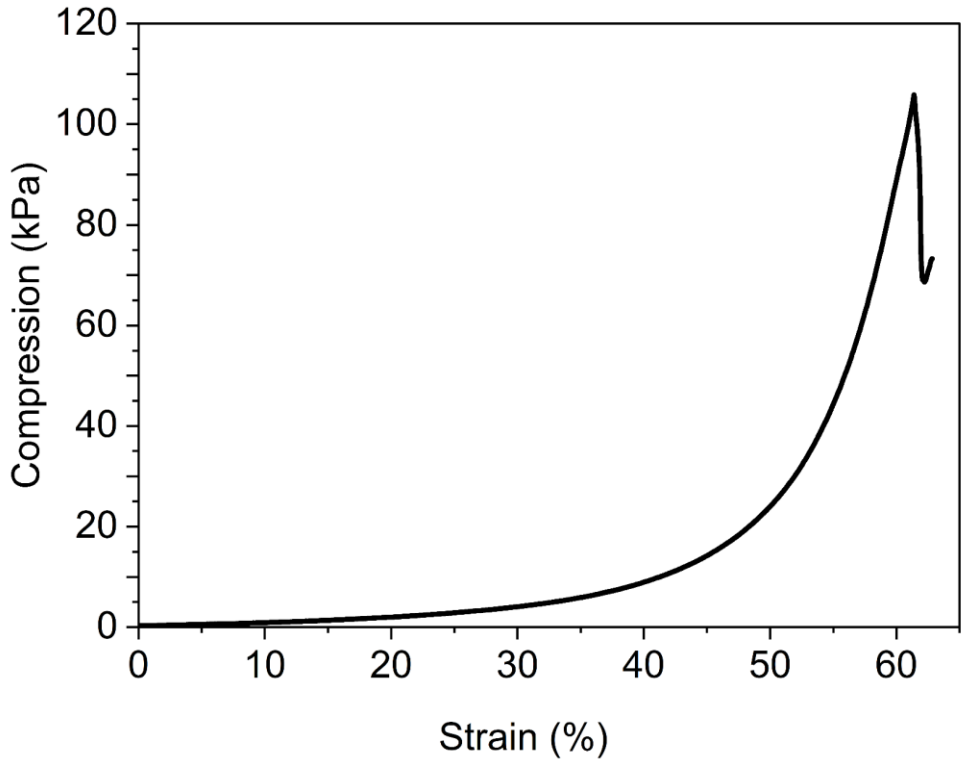

Figure S4. The compression force of the PAAm hydrogel is used as a model of nucleus pulposus tissue during MS and MSP injection.

6. In vitro evaluation of NPC on MS and MSP

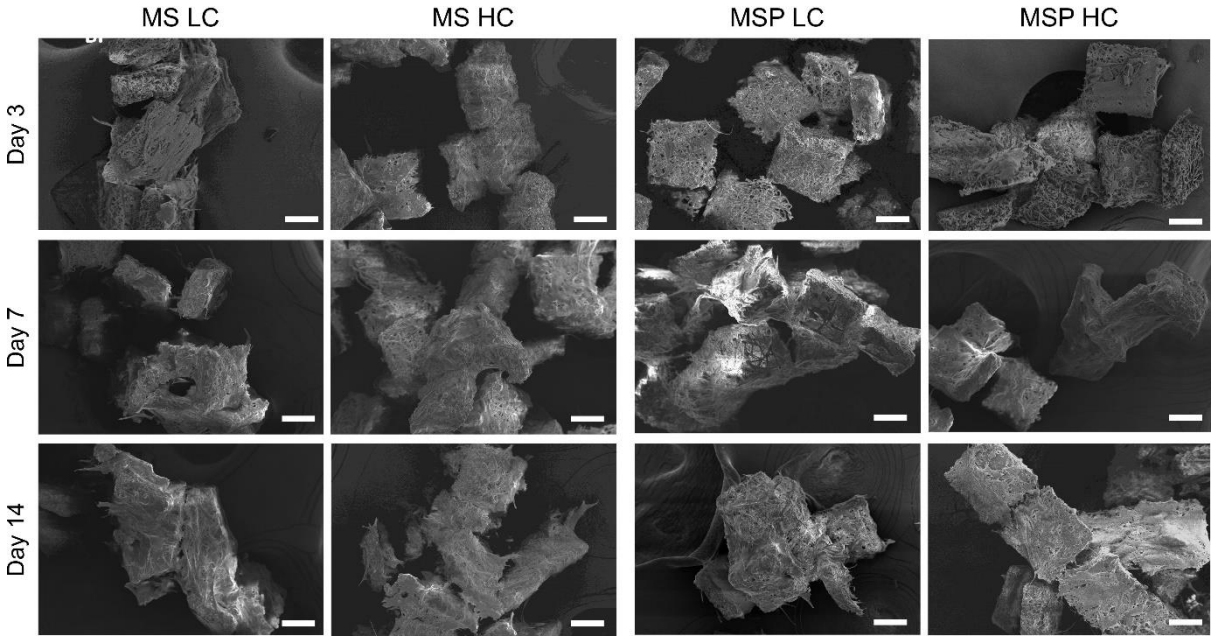

Figure S5. SEM images of MSs and MSPs on days 3, 7, and 14 of NPC culture. Scale bar: 50 μm.

7. TF hydrogel morphology

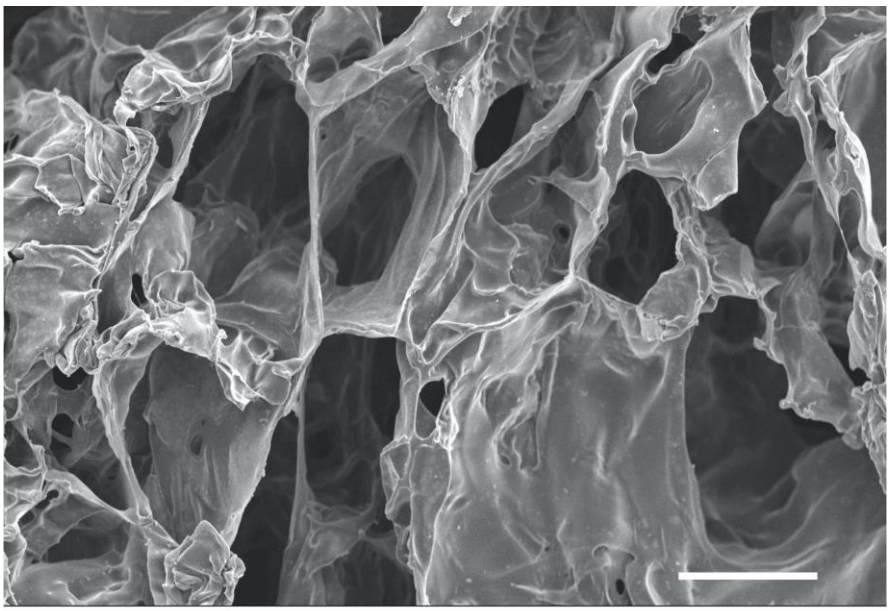

Figure S6. SEM image of pure TF hydrogel. Scale bar: 100 μm.

8. Wettability of the microscaffolds

The contact angles for porous microscaffolds (MSP) and microscaffolds (MS) are 95° ± 10° and 105°± 6°, respectively. The contact angle for PLGA as spun nanofibrous mat is 130°± 4°. This demonstrates that there is no significant difference between MSP and MS, however both groups have enhanced hydrophilicity compared to nanofibrous mat, which is conducive to better cell adhesion.

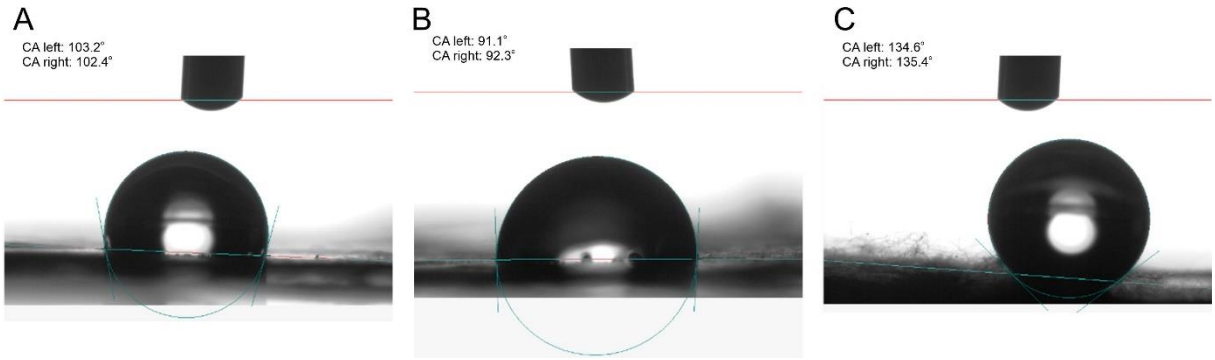

Figure S7. The representative images of contact angle for the A) microscafolds without additional pores (MS), B) porous microscafolds (MSP), and C) nanofibrous PLGA material.

9. TF-hydrogel stiffness measurements

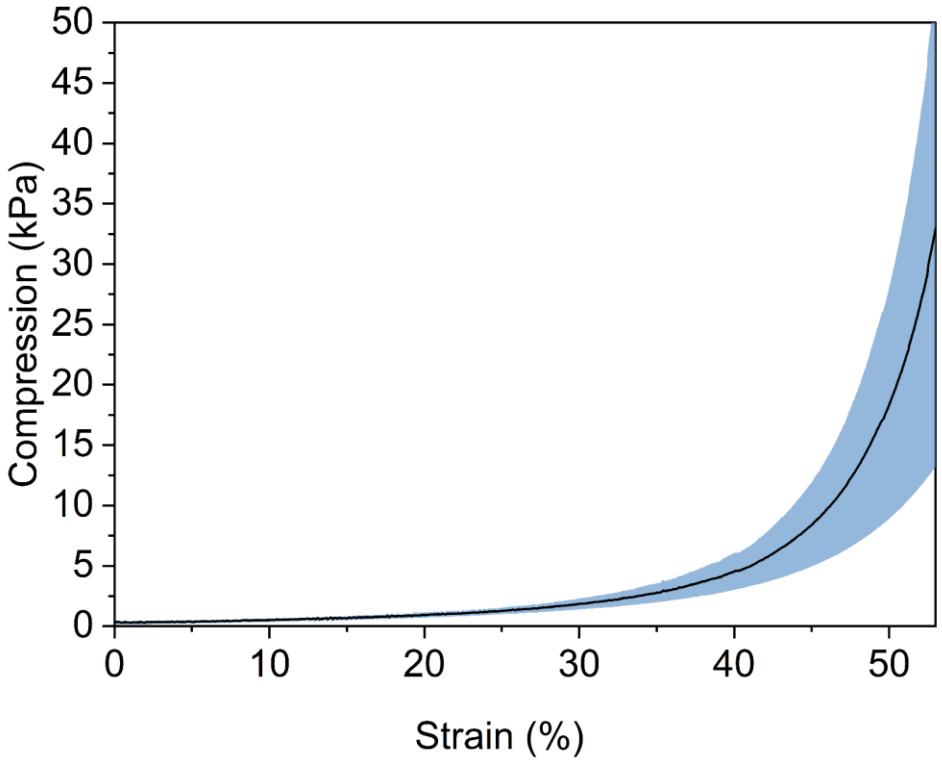

Figure S8. The compression force of the TF hydrogel is used as a model of nucleus pulposus tissue for 3D cell culture.